Quenching efficiency of pyrene fluorescence by nucleotide monophosphates in cationic micelles

ARTICLE *in* JOURNAL OF PHOTOCHEMISTRY AND PHOTOBIOLOGY A CHEMISTRY · FEBRUARY 2009

Impact Factor: 2.5 · DOI: 10.1016/j.jphotochem.2008.10.028

4 AUTHORS:

Francesca Cuomo
Università degli Studi del Molise
28 PUBLICATIONS **259** CITATIONS
SEE PROFILE

Gerardo Palazzo
Università degli Studi di Bari Aldo Moro
151 PUBLICATIONS **2,002** CITATIONS
SEE PROFILE

Andrea Ceglie
Università degli Studi del Molise
121 PUBLICATIONS **1,825** CITATIONS
SEE PROFILE

Francesco Lopez
Università degli Studi del Molise
59 PUBLICATIONS **617** CITATIONS
SEE PROFILE

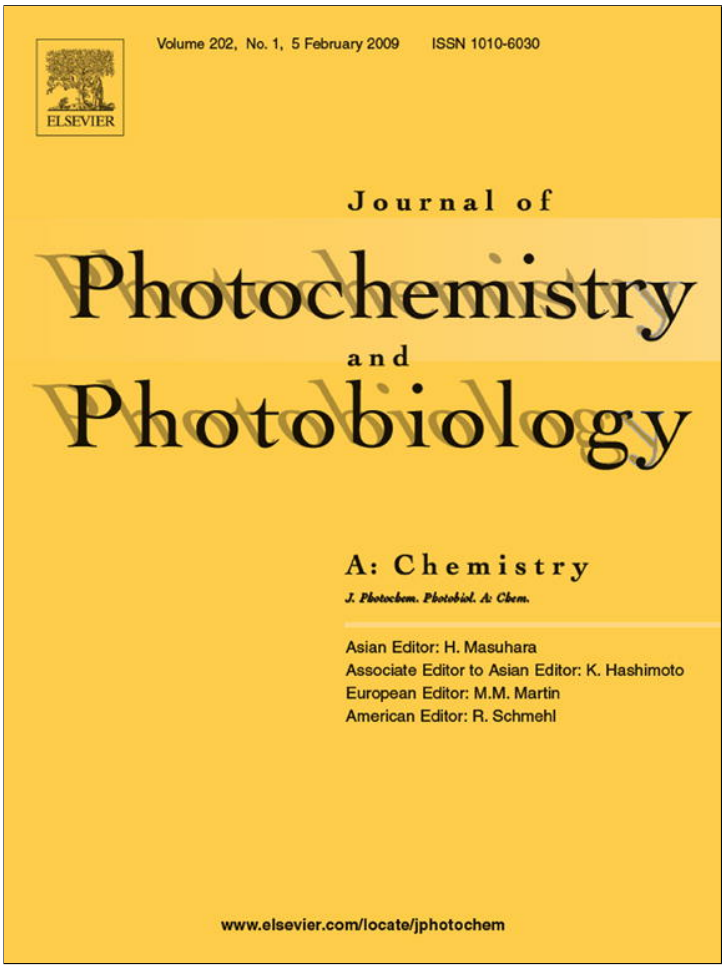

Journal of Photochemistry and Photobiology A: Chemistry 202 (2009) 21–27

Contents lists available at ScienceDirect

Journal of Photochemistry and Photobiology A: Chemistry

journal homepage: www.elsevier.com/locate/jphotochem

Quenching efficiency of pyrene fluorescence by nucleotide monophosphates in cationic micelles

Francesca Cuomo[a], Gerardo Palazzo[b], Andrea Ceglie[a], Francesco Lopez[a,*]

[a] Consorzio Interuniversitario per lo sviluppo dei Sistemi a Grande Interfase (CSGI), c/o Department of Food Technology (DISTAAM), Università del Molise, I-86100 Campobasso, Italy

[b] Consorzio Interuniversitario per lo sviluppo dei Sistemi a Grande Interfase (CSGI), c/o Department of Chemistry, Università di Bari, I-70126 Bari, Italy

ARTICLE INFO

Article history:
Received 2 July 2008
Received in revised form 24 October 2008
Accepted 31 October 2008
Available online 21 November 2008

Keywords:
Fluorescence quenching
Nucleotides
Cationic micelle
Counter ion
Zeta potential

ABSTRACT

The fluorescence behaviour of pyrene solubilized in the hexadecyltrimethylammonium bromide (CTAB) aqueous micellar solution in the presence of different nucleotide-monophosphates (NMPs) was investigated by monitoring the quenching and dequenching of pyrene steady-state fluorescence.

The data clearly show that diverse nucleotide-monophosphates influence in different way the fluorescence of micellized pyrene: guanosine 5′-monophosphate (GMP), uridine 5′-monophosphate (UMP) and thimydine 5′-monophosphate (TMP) lead to a reduction in fluorescence intensity (quenching), while adenosine 5′-monophosphate (AMP) and cytosine 5′-monophosphate (CMP) induce an increment in pyrene fluorescence (dequenching). For all the NMPs the photophysical effect saturates at concentration higher than 40 mM. In the absence of micellar solution the fluorescence of pyrene follows the typical linear behaviour according to the Stern–Volmer relation.

The quenching and dequenching efficiencies were analyzed according to a recently proposed model, based on the assumption that the anionic nucleotides compete with the surfactant counterion (bromide) for micelle surface. Results make available the follows of quenching efficiency order (GMP > UMP > TMP) and dequenching efficiency order (AMP > CMP).

Zeta-potential measurements confirm that the predominant interaction occurs between the positively charged micellar surface and the negatively charged phosphate moieties on the nucleotides. The collected results clearly show that the fluorescence of pyrene solubilized in the CTAB micellar solution can be reduced (quenched) or enhanced (dequenched), depending on the chemical properties of the nucleobase.

1. Introduction

In the last few years, the studies on interactions between DNA and self-assembled nanostructures, such as micelles and vesicles, have been of major concern, due to the possibility to use these complexes as transfection tools [1]. In particular, the interaction between amphiphilic molecules and biological polyelectrolytes, like that occurring between DNA and cationic surfactant systems, has received special attention [2,3]. Among the technological applications, the use of micellar systems for the study of synthetic nucleolipids is recently coming up [4–7].

Since the modern biotechnology is focused on the development of new tools for DNA sequence analysis and DNA detection, functional for the improvement of automated DNA sequencing [8], the study of the interactions between polynucleotides and cationic surfactants, can add significant information, as to the recognition, sensing and supramolecular chemistry [9]. The electrostatic interactions between the positively charged surface of micelles formed by cationic surfactant and the negatively charged mononucleotides are expected to lead to the formation of complexes. A study of the affinity of mononucleotides for the micellar wall could be thus useful for the analysis of the compaction behaviour of polynucleotides and for some applications involving surfactant-mononucleotide interactions (e.g. mononucleotide determination by means of capillary electrophoresis) [10]. Schematically, micelles are composed of a hydrocarbon-like core and a headgroup region, containing charged (or polar) surfactant headgroups, counterions, and water. The micelles made by the single-tailed cationic surfactant CTAB are considered the archetype of cationic micelles. One of the most fundamental properties of aqueous micellar solutions is their ability to solubilize a wide variety of organic solutes with quite distinct polarities and degrees of hydrophobicity [11].

Fluorescence quenching has been widely employed as a source of information about biochemical systems. Static quenching, for example, has often been investigated in order to detect whether the fluorophore and the quencher may have a stacking interaction. Such interactions often occur between purine and pyrimidine nucleotides and a number of fluorophores [12,13]. Interactions

* Corresponding author. Tel.: +39 0874404632; fax: +39 0874404652.
E-mail address: lopez@unimol.it (F. Lopez).

1010-6030/$ – see front matter © 2008 Elsevier B.V. All rights reserved.
doi:10.1016/j.jphotochem.2008.10.028

between nucleotides and fluorophores, like coumarin, were extensively studied to develop a method for DNA sequencing using a single electrophoretic lane for all nucleotides [8]. A mechanisms of quenching of polynuclear aromatic dye fluorophores bound to DNA, involved with an electron transfer mechanism with the photoexcited dyes acting as electron acceptor, was firstly reported by the group of Kittler in aqueous systems [14,15]. Later, Geacintov et al. confirmed this electron transfer mechanisms by studying the fluorescence quenching of polynuclear aromatic hydrocarbon-based dyes by DNA bases [16,17]. Studies based on quenching of pyrene fluorescence by suitable molecules have been also extensively used to probe the association properties of the quencher with micelles [18–23]. Pyrene was broadly used as a fluorescent probe to investigate several aspects of micellar features [24–28]. In a recent contribution [29] we reported that although similar in chemical structure, AMP and UMP influence the fluorescence of pyrene secluded in CTAB micelles oppositely. In the present work, the quenching and dequenching ability of the following series of NMPs: AMP, GMP, UMP, CMP and TMP is analyzed by following the fluorescence of pyrene solubilized in CTAB micelles. The application of the previously proposed model based on a saturation process of the micellar wall led us to compare the behaviour of the diverse nucleotide-monophosphates here investigated and highlight their different quenching abilities.

2. Experimental

2.1. Chemicals

AMP (≥99%, disodium salt), UMP (>99%, disodium salt), CMP (>99%, disodium salt) GMP (>99%, disodium salt), TMP (≥99%, disodium salt), CTAB (≥99%), Uridine (≥99%), Tris–hydrochloride and pyrene were from Sigma. CTAB was three times re-crystallized from anhydrous ethanol, and stored over dried silica gel under vacuum. All the experiments were performed in a 10-mM Tris–HCl pH 7.5 buffer solution.

2.2. General procedures

Solutions were prepared by adding suitable amounts of the components in volumetric flasks; pyrene was added as methanol solution. The final concentration of methanol in all samples was 1 vol.%. For all the micellar solutions the final concentration of pyrene was 5×10^{-7} M (the aqueous solubility of pyrene is 3.9×10^{-7} M [30]). All fluorescence measurements were performed using a Varian Eclipse spectrofluorimeter in a 1-cm quartz fluorescence cuvette, at 25 °C. The measurements were performed after an incubation time of 30 min. The excitation and the emission slit-width were 5 mm. The excitation and the emissions wavelengths utilized for this study were 334 nm and 374 nm, respectively.

For the zeta-potential measurements the electrophoretic mobilities of the species in the micellar system were determined by laser Doppler velocimetry using a Zetasizer Nano ZS90 (Malvern, UK). The zeta potential of micelles was calculated from their electrophoretic mobility by means of the Smoluchowski approximation of the Henry equation [31]. Samples of CTAB micelles (2 mM) containing variable NMPs concentrations were injected in dedicated disposable capillary cells. All measurements were performed at 25 °C.

3. Results and discussion

3.1. Steady-state quenching of pyrene in aqueous buffer

Steady-state quenching experiments were performed in buffer solutions and in CTAB micelles using pyrene as fluorescent probe. In order to investigate the role of the surfactant on pyrene fluorescence, we firstly examined the behaviour of the dye in the presence of NMPs in aqueous buffer solution. For pyrene dissolved in aqueous buffer we can easily assume that the quenching results from the random encounters between pyrene and nucleotides [32–35]. Under such an assumption, the drop of fluorescence (quenching) can be analyzed according to general mechanisms that take into account the complex formation in the ground state as well as in the excited state. As well known, the variation of fluorescence intensity is related to the concentration of the quencher by the Stern–Volmer equation (Eq. (1)):

$$\frac{F_0}{F} = 1 + K'_{SV}[Q] \quad (1)$$

where F and F_0 are the fluorescence intensities in the presence and in the absence of quencher respectively, [Q] indicates the quencher concentration and K'_{SV} represents the Stern–Volmer constant which has dimensions of reciprocal concentration. In Fig. 1, we show the series of Stern–Volmer plots obtained in aqueous buffer solution containing pyrene (without CTAB) in the presence of NMPs. As illustrated in Fig. 1 and according to Eq. (1), the ratio F_0/F is linearly dependent on the NMPs concentration and a considerable difference between the nucleotides in terms of K'_{SV} is evident (see also Table 1). The quenching efficiency was found to increase in the following order: TMP > GMP ≈ UMP > CMP > AMP ranging from a maximum value of K'_{SV} (TMP = 352 M^{-1}) to a minimum (AMP = 10 M^{-1}). Although redox potentials of nucleosides in water are not well established (due to their irreversible oxidation in aqueous media) and some details are still not fully resolved, there is a general consensus on the idea that the quenching of pyrene emission by nucleosides, nucleotides and nucleic acids occurs via a photoinduced electron transfer [34,36].

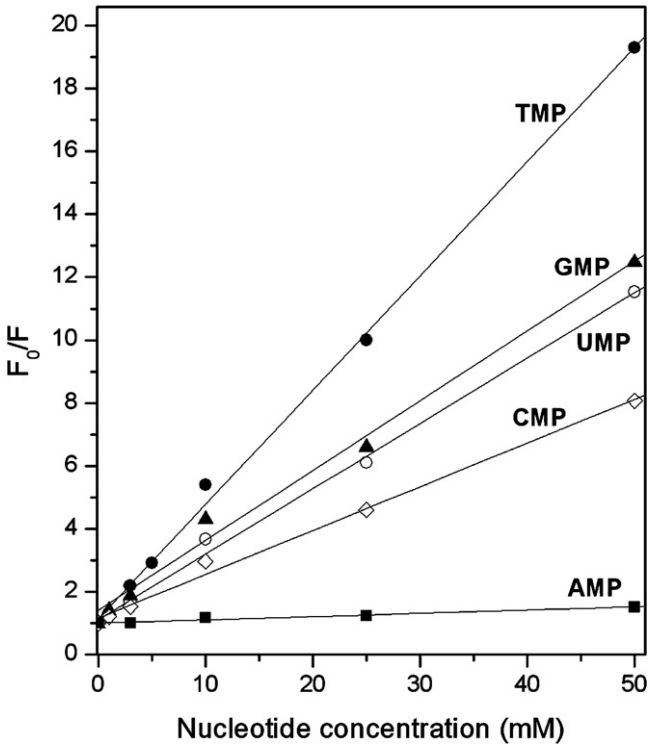

Fig. 1. Stern–Volmer plots (emission 374 nm). F_0/F as function of nucleotide monophosphate concentration in aqueous solution at pH 7.5 (10 mM Tris–HCl) (excitation 334 nm). (■) AMP, (○) UMP, (▲) GMP, (◊) CMP, (●) TMP. The straight lines are the linear regression according to Eq. (1) (correlation coefficients: AMP r^2 = 0.982, UMP r^2 = 0.991, GMP r^2 = 0.993, TMP r^2 = 0.990, CMP r^2 = 0.995); the best fit K'_{SV} values are listed in Table 1.

Table 1
Parameters describing the effect of NMPs on the fluorescence of pyrene solubilized in aqueous buffer (10 mM Tris–HCl pH 7.5) and in CTAB micellar solutions.

	CTAB			Buffer
	K_{SV}^{APP}	K_L (M^{-1})	K^{Br} [Br^-]	K'_{SV} (M^{-1})
AMP	–	205 ± 30	0.3 ± 0.02	10 ± 1
GMP	3.55 ± 0.15	565 ± 60		232 ± 6
CMP	–	151 ± 30	0.18 ± 0.02	144 ± 4
TMP	0.46 ± 0.06	152 ± 60		352 ± 11
UMP	0.66 ± 0.04	325 ± 50		211 ± 6

According to the work of Seidel et al. [8], the data of Table 1 are accounted for by assuming that TMP and UMP are more easily reduced by the photoexcited pyrene than AMP and CMP in agreement with the reported redox potentials for nucleobases [8]. The case of GMP is somehow different because the quenching of pyrene fluorescence is possible only through GMP oxidation [8].

3.2. Steady-state quenching of pyrene in micellar solution

We have previously shown that, notwithstanding the akin chemical structure, AMP and UMP influence the fluorescence of pyrene secluded in CTAB micelles oppositely [29]. In the present work, the investigation was extended to the following series of NMPs: AMP, GMP, TMP, CMP and UMP. The spectra displayed in Fig. 2 are typical of pyrene solubilized in a 2-mM CTAB micellar solution loaded with different NMPs (10 mM final concentration). The fluorescence intensity of pyrene clearly decreases in the presence of GMP, UMP and TMP, while increases in the presence of AMP and CMP. It is worth noting that the ratio between emissions at different wavelengths remains constant, suggesting that the polarity of pyrene surroundings is unaffected by NMPs loading (polarity index I(I)/I(III) ≈ 1.1). Furthermore, pyrene within micelles is readily available to quenchers, as demonstrated by several studies [37] and is believed to be localized in the "palisade" of the micelle [26]. In Fig. 3, the dependencies of fluorescence intensity (emission at 374 nm) on the NMPs concentration (0–100 mM) for the total series of NMPs are reported. The NMP-specific effect saturates at high nucleotide concentrations. Since the ratio between the fluorescence intensity in the absence of NMPs and the fluorescence in presence of NMP does not depend linearly on NMP concentrations, but clearly follows a saturation trend, we used a previously proposed model for treating our data [29]. Briefly, we start from the assumption that bromide ions act as quencher for the pyrene secluded in micelles and that the final photophysical effect of NMP addition depends on the competition between Br^- and NMP^- for the micellar binding sites. The bromide and NMP ions interact with the positively charged micellar surface, as shown below:

$$Br^- + S^+ \rightleftarrows Br - S \quad \text{and} \quad NMP^- + S^+ \rightleftarrows NMP - S$$

where S^+ indicates the adsorption sites available for the adsorbate on the micellar surface. The interaction between anions and CTAB micelles may be treated as classical Langmuir adsorption isotherms:

$$\frac{[Br - S]}{[Br^-][S^+]} = K_L^{Br} \quad \text{and} \quad \frac{[NMP - S]}{[NMP^-][S^+]} = K_L^{NMP}$$

where K_L^i stands for the Langmuir's constant for *i*-th species. The competition between bromide and NMP is given by the constraint: $[S_T] = [S^+] + [Br–S] + [NMP–S]$, where $[S_T]$ denotes the concentration of total adsorption sites. This formalism is equivalent to the competitive binding of two ligands for the binding sites of a macromolecule (in such a case K_L^{Br} and K_L^{NMP} stands for the respective binding constant). Of course, the adsorption/binding of the *i*-th

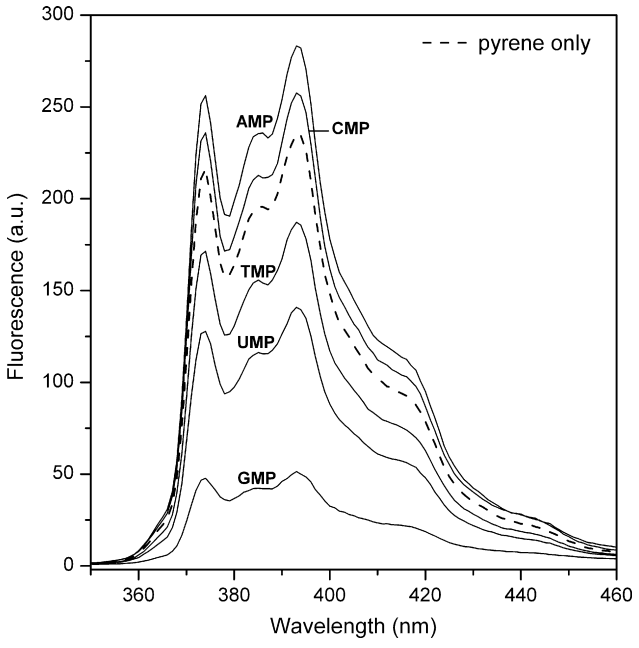

Fig. 2. Fluorescence emission spectra of pyrene (5×10^{-7} M) solubilized in 2 mM CTAB micellar solution at pH 7.5 (10 mM Tris–HCl) upon addition of 10 mM AMP, GMP, UMP, CMP and TMP (excitation 334 nm).

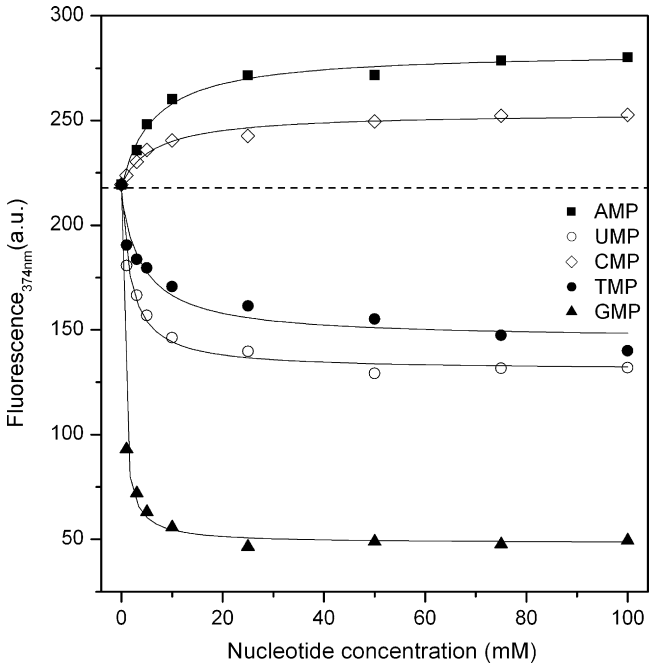

Fig. 3. Fluorescence intensities of pyrene at 374 nm (excitation 334 nm) as function of nucleotides concentration in a 2-mM CTAB micellar solution at pH 7.5 (10 mM Tris–HCl). (■) AMP, (○) UMP, (▲) GMP, (◊) CMP and (●) TMP. The AMP and CMP data have been fitted to Eq. (4) while the TMP, UMP and GMP data have been fitted to Eq. (5).

species to micelles leads to observable fluorescence effects only if the micelle contains pyrene. Thus, the contribution of a species to the observed fluorescence quenching is given by the concentration of NMP adsorbed to the micelles *times* the fraction of micelle containing pyrene (the ratio of pyrene to micelle concentration).

The concentration of total binding sites for the quencher is proportional to the micelle concentration and, in a first order approximation, each surfactant head represents a potential binding site ($[S_T] \approx N_{agg} \times$ (micelle concentration) $\approx$ [CTAB]; N_{agg} being the surfactant aggregation number). Starting from this assumption the Stern–Volmer relation (Eq. (1)) develops into

$$\frac{F_0}{F} = 1 + \frac{K_{SV}^{Br}[Br^-]K_L^{Br} + K_{SV}^{NMP}[NMP]K_L^{NMP}}{1 + K_L^{Br}[Br^-] + K_L^{NMP}[NMP]} \quad (2)$$

where the *adimensional* K_{SV}^i constants include the pyrene concentration and the micelle aggregation number ($K_{SV}^i = K'_{SV^i} N_{agg}[pyrene]$). The previous work [29] indicates that for a 2-mM CTAB micellar solution $1 + K_L^{Br}[Br^-] \approx 1$.

Considering the previous adjustment Eq. (2) can be rewritten as

$$\frac{F_0}{F} = 1 + \frac{K^{Br}[Br^-] + K_{SV}^{NMP}[NMP]K_L^{NMP}}{1 + K_L^{NMP}[NMP]} \quad (3)$$

where $K^{Br} = K_L^{Br}\ K_{SV}^{Br}$. Eq. (3) well describes the effect on pyrene fluorescence of the competition between NMPs and bromide ions for the adsorption sites on the micellar surface. The different (quenching and dequenching) behaviour for different NMPs should be mainly traced out to their different photophysical properties: $K_{SV}^{NMP} \approx 0$ (NMP does not quench pyrene fluorescence) and $K_{SV}^{NMP} > K_{SV}^{Br}$ (NMP is a good quencher for pyrene).

The fluorescence *enhancement* upon NMPs loading (observed for AMP and CMP) were fitted to the following equation obtained from Eq. (3) under the assumption $K_{SV}^{NMP} \approx 0$.

$$F = F_0 \left(\frac{1 + K_L^{NMP}[NMP]}{1 + K^{Br}[Br^-] + K_L^{NMP}[NMP]} \right) \quad (4)$$

In these cases F_0 values are the limit values obtained with the complete displacement of the quencher Br^- from the micellar surface as illustrated in Scheme 1. The scenario of fluorescence quenching unproductive NMP displacing the quencher Br^- from the micellar surface is supported by the evidence that pyrene fluorescence in micelle of CTAC (i.e. where Br^- is substituted by Cl^-) is 40% higher than that observed in CTAB and that in the case of CTAC micelles the enhancement in fluorescence due to AMP is less than 10% (not shown). Since bromide acts as a quencher, the experimental fluorescence value in absence of NMPs does not correspond to the true values of the pyrene fluorescence without a quencher (F_0). Instead it corresponds to F_0^{APP}, i.e. the fluorescence of sample without the nucleotide contribution but still in the presence of Br^-.

In the case of NMPs (GMP, UMP and TMP) that successfully quench the pyrene fluorescence ($K_{SV}^{NMP} \neq 0$) we can describe the fluorescence behaviour in terms of the pyrene fluorescence in absence of NMP (but still in the presence of Br^-) according to

$$F = F_0^{APP} \left(\frac{1 + [NMP]K_L^{NMP}}{1 + K_L^{NMP}[NMP](1 + K_{SV}^{APP})} \right) \quad (5)$$

where $K_{SV}^{APP} = \frac{1+K_{SV}^{NMP}}{1+K^{Br}[Br^-]} - 1$

Although developed to describe the influence of UMP and AMP on pyrene fluorescence in CTAB micelles, the above formulation holds also for the total series of NMPs explored in the present work. Actually, Eqs. (4) and (5) nicely fit the data of Fig. 3 and the best fit parameters are listed in Table 1. For all the NMPs the saturation in their photophysical effect (either quenching either dequenching) on pyrene fluorescence is consistently described by adsorption isotherms characterized by Langmuir's constants of the same order of magnitude. Independent zeta-potential experiments, to be described in the next section, fully confirm the adsorption of NMPs on the micellar wall thus verifying the validity of the binding isotherm at the basis of the above described treatment.

The comparison between the Stern–Volmer constants measured in absence of micelles (K'_{SV}) and the parameter K_{SV}^{APP} reflecting the quenching efficiency in micelle is interesting. For AMP, the ansatz $K_{SV}^{NMP} \approx 0$ reasonably holds and consistently it acts as a dequencher of pyrene fluorescence in micelles; on the other hand, K'_{SV} of CMP is ten times larger but CMP loading still induces a weaker enhancement of fluorescence in micelles (see Fig. 3). Otherwise, UMP acts as a quencher in micellar solution although in buffer solution it has a K'_{SV} that is only twice that of CMP. The order of quenching efficiency in buffer solutions is not preserved in micellar solutions where GMP shows a much higher quenching efficiency than UMP and TMP (see Table 1 and the plateau levels of Fig. 3). From a formal point of view these results indicate that the Stern–Volmer constants K'_{SV} in buffer solution and at the micelle interface are different, but about the molecular origin of this discrepancy we can only speculate. The quenching of pyrene fluorescence by NMPs is due to a photoinduced electron transfer [8] and this is expected to be intimately correlated to proton transfer processes [34]. The presence of the charged micellar interface could heavily affect the pK_as and thus the protonation state of the purine and pyrimidine bases. In addition, for micelles made of cationic surfactants (such as CTAB) the local pH (at the interface) may be 1–2 units higher than its value in solution [38] and this of course precludes a simple comparison with the reactivity in buffer solution. Finally we note that the electric field within the Stern's layer could strongly influence the electron transfer reaction. This last point could have some relevance to explain the high yield of pyrene* quenching by GMP in micelles because in such a case the electron transfer from the anionic GMP to the pyrene* located at the cationic micellar surface should be favoured.

3.3. Zeta-potential measurements

To get insight into the mechanism underlying the NMPs–pyrene interactions in the micellar system, the role of the positively charged interface on pyrene fluorescence quenching was investigated by zeta-potential measurements. All the NMPs are anions and are thus expected to strongly interact with the cationic surfactant. We have previously demonstrated that there is no substantial difference in micellar size whether the anion added is the purine-based nucleotide AMP or the pyrimidine-based nucleotide UMP. It was thus concluded that the opposite photophysical effect exerted by AMP and UMP was unrelated to any change in the micellar microstructure [29]. The zeta-potential value gives indications about the potential difference between the dispersion medium and the stationary layer of fluid attached to the dispersed particle and thus probes directly the binding of charged species to the micelles. Fig. 4 shows the electrophoretic behaviour of CTAB micelles obtained by measuring zeta-potential values as function of NMPs concentration. In the absence of NMPs the zeta potential is positive (ζ = +70 mV) as expected for cationic micelles. For all the nucleotides, the addition of NMPs, results in a drastic decrease of the initial zeta-potential value and the maximal reduction is reached at 40 mM of NMPs (the same concentration where the photophysical effect of NMP saturates) thus demonstrating the adsorption of anionic NMPs at the micellar surface. The adsorption isotherms probed by zeta-potential measurements of Fig. 4 are well described by the Langmuir's isotherm [39]:

$$\zeta = \zeta_0 + \frac{\zeta_\infty K_L[NMP]}{1 + K_L[NMP]} \quad (6)$$

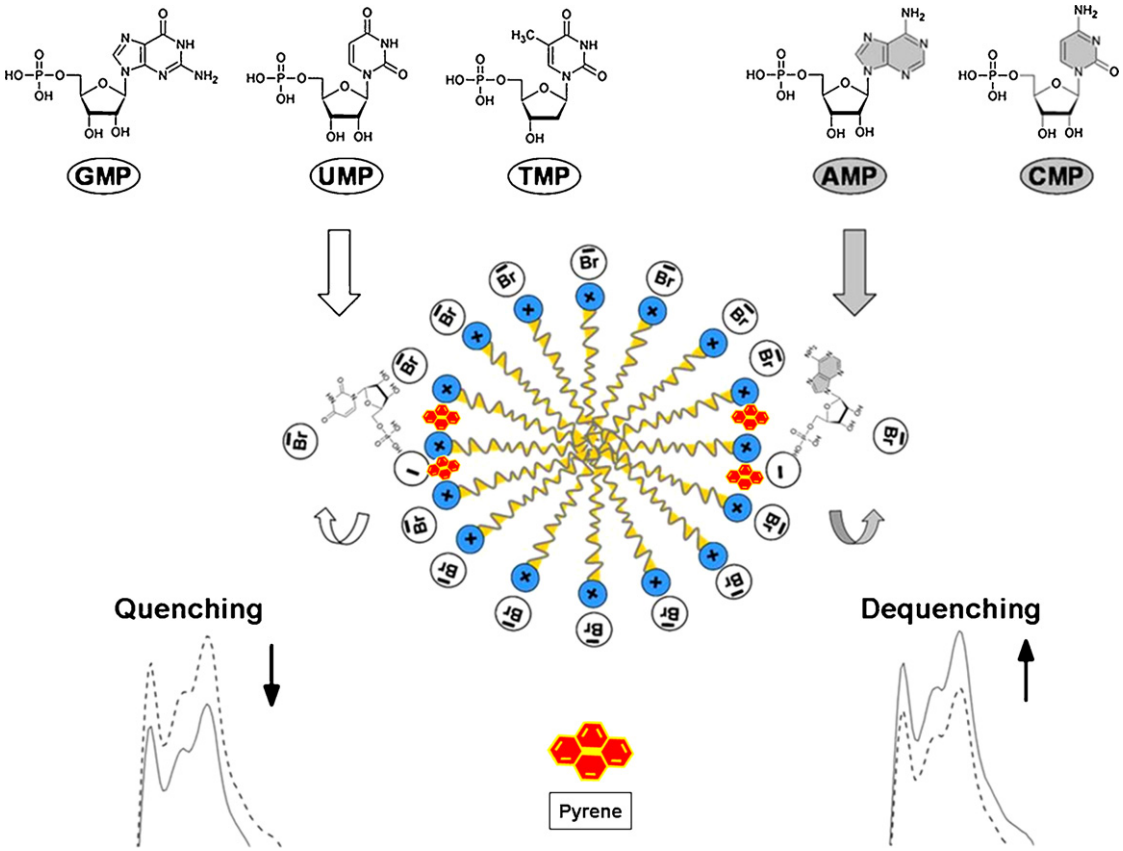

Scheme 1. Schematic representation of the photophysical response due to counter ion switch. The scheme shows that all nucleotides concentrate on the micellar interface replacing the bromide counter ions. GMP, UMP and TMP lead to a reduction in the pyrene fluorescence intensity because have a quenching efficiency higher than bromide counter ion. AMP and CMP induced an increment in the pyrene fluorescence because they are less effective than the bromide counter ion. On the top of the scheme the chemical structures of the complete series of NMPs utilized in this work are shown. The aromatic rings of NMPs with quenching abilities are reported in white while the aromatic rings of NMPs with dequenching abilities are reported in grey. On the bottom of the scheme the black dashed line refers to the pyrene fluorescence emission spectrum without NMPs. The grey continuos line refers to the pyrene fluorescence emission spectrum in the presence of NMPs.

where ζ_0 and ζ_∞ are the zeta-potential values of the micelle without NMP and after saturation with NMP, respectively and K_L is the Langmuir's constant. However, the poor quality of ζ-values (compared to the fluorescence data) results in an high uncertainty associated to the K_L values (around 100%) and to demonstrate the consistency of the independent zeta potential and fluorescence experiments we prefer to fit the data to Eq. (6) imposing the K_L values obtained from fluorescence quenching experiments (Table 1) and leaving only ζ_0 and ζ_∞ as free parameters. As shown in Fig. 4, NMP-induced decays of the zeta potential agree with the adsorption isotherms inferred by the analysis of fluorescence data reported in Fig. 3. The consistency of the two different sets of measurements validates the physical ground of the model proposed to analyze the fluorescence response upon NMP loading. The values of Langmuir's constant for different NMPs have the same order of magnitude indicating that the adsorption to the micellar surface is mainly due to the contribution of the phosphate moiety; likely through electrostatic interactions with the cationic surfactant head.

3.4. Steady-state quenching of pyrene by uridine

The results discussed in the above sections suggest different roles of the NMP moieties on the response of the pyrene fluorescence to nucleotides loading. The negatively charged phosphate group drives the adsorption of NMPs to the micellar surface and leads to the saturation of the photophysical effects while the properties of the nucleobases (in the peculiar environment of micellar surface) dictate the phenomenology of the fluorescence response (quenching versus dequenching). In order to further confirm the role of the phosphate group on the observed pyrene* quenching, we have investigated the effects of uridine (the nucleoside present on UMP) on pyrene fluorescence. Fig. 5 shows the Stern–Volmer plot obtained on micellar solutions of pyrene upon loading of Uridine or of UMP. The dependence of the Stern–Volmer ratio on uridine concentration shows the linear behaviour distinctive of the Stern–Volmer equation instead of the saturation curve observed upon UMP loading. The data of Fig. 5 confirm that the saturation behaviour observed for NMPs is due to the presence of the anionic phosphate group; uridine has not well-defined binding sites on the micelles. At low quencher concentration UMP exhibits a quenching efficiency higher than uridine because, due to the electrostatic driven adsorption, the nucleotide local concentration is higher than that of the corresponding nucleoside. At high quencher concentration (>80 mM) uridine and UMP share the same quenching efficiency. This evidence rules out the possibility that the pyrene* quenching by uridine involves only the fraction of pyrene dissolved in the aqueous bulk because in this case we should still observe the fluorescence of micellized pyrene.

The present study demonstrates that pyrene quenching behaviour reflects the specific donor–acceptor relationship of the fluorophore with the different functional groups of the NMPs used. Moreover, the quenching model applied emphasizes the contribution of the counter ion bromide to the quenching mechanism. Accordingly, the differences in fluorescence quenching found in the micellar solution in the presence of NMPs are likely related to a switch of counterion that takes place in these sys-

tems and thus reflect changes in the specific micelle–counter ion interaction. The hypothesized mechanism of the "counter ion switch" underlying the quenching/dequenching effect of the five nucleotide-monophosphates studied is depicted in Scheme 1. Both mechanism of quenching (GMP, UMP, and TMP) and dequenching (AMP, CMP) are based on the capability of the different NMPs to dislodge the bromide ions. Noticeably, this experimental evidence could be helpful in biological issues, since the different types of interaction between NMPs and the positively charged surfactant

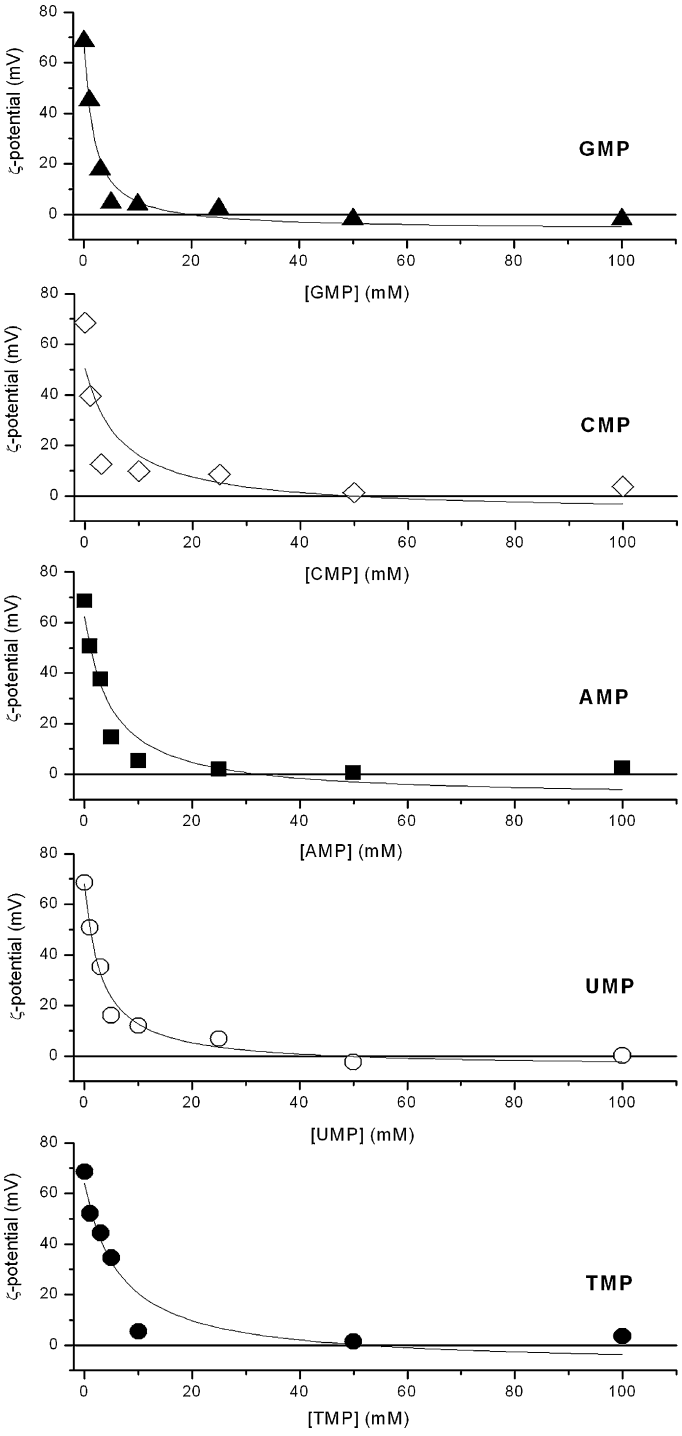

Fig. 4. *Z*-potential of 2 mM CTAB micellar solutions at pH 7.5 (10 mM Tris–HCl) loaded with different nucleotide monophosphate. The points represent the experimental values, the curves are the best fit according to Eq. (6) imposing the K_L values of Table 1 (evaluated from the fluorescence data of Fig. 3).

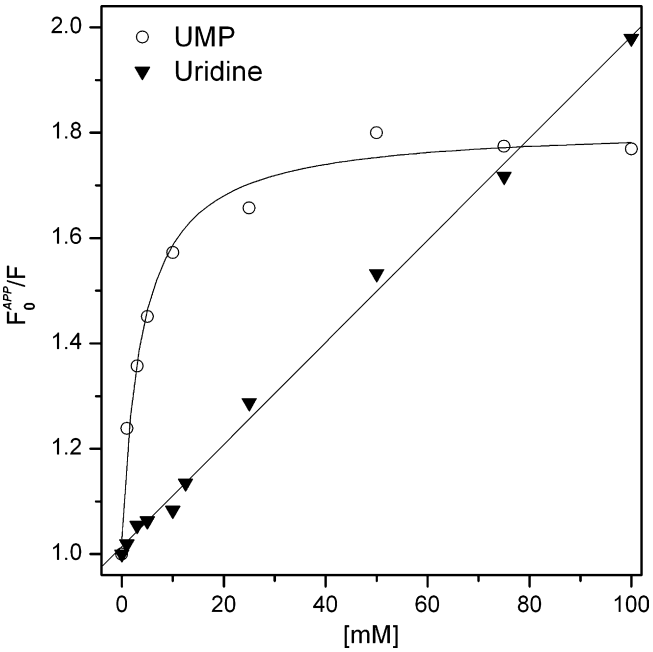

Fig. 5. Stern–Volmer plots (emission 374 nm; excitation 334 nm). F_0^{APP}/F vs. UMP (○) and Uridine (▼) concentration in a 2-mM CTAB micellar solution at pH 7.5; the ordinate F_0^{APP}/F represents the ratio between the emission in absence (F_0^{APP}) and in the presence of UMP or uridine.

could represent the basis for a suitable method to selectively recognize the different NMPs in aqueous solutions.

4. Conclusion

In this paper, the quenching efficiencies of pyrene solubilized in CTAB micellar solution by NMPs were studied. The data presented indicate that NMPs influence in different way the fluorescence of micellized pyrene. Remarkably, GMP, UMP and TMP act as quenchers and AMP and CMP act as dequenchers. The quenching efficiency follows the scale GMP > UMP > TMP while the dequenching efficiency follows the scale AMP > CMP. As a whole, the data collected were successfully accounted for by assuming that the NMPs compete with the surfactant counterion (bromide) for the surface of the micelle. The present data could also be highly valuable for sensing applications allowing the use of simple spectrofluorimetric assays for the determination of species that do not have any influence on the fluorescence of the micellized probe.

Acknowledgments

This work was supported by the Italian Ministero Università Ricerca (PRIN 2006: "Self-assembling nanosystems with DNA-like addressability") and by Consorzio Interuniversitario per lo sviluppo dei Sistemi a Grande Interfase (CSGI-Firenze).

References

[1] R.S. Dias, A.A.C.C. Pais, M.G. Miguel, B. Lindman, Colloids Surf. A 250 (2004) 115.
[2] R. Dias, S. Mel'nikov, B. Lindman, M.G. Miguel, Langmuir 16 (2000) 9577.
[3] M. Cardenas, A. Braem, T. Nylander, B. Lindman, Langmuir 19 (2003) 7712.
[4] D. Berti, F. Pini, P. Baglioni, J. Phys. Chem. B 103 (1999) 1738.
[5] D. Berti, P. Baglioni, S. Bonaccio, G. Barsacchi-Bo, P.L. Luisi, J. Phys. Chem. B 102 (1998) 303.
[6] R. Angelico, A. Ceglie, F. Cuomo, C. Cardellicchio, G. Mascolo, G. Colafemmina, Langmuir 24 (2008) 2348.
[7] F. Cuomo, F. Lopez, R. Angelico, G. Colafemmina, A. Ceglie, Colloid Surf. B 64 (2008) 184.
[8] C.A.M. Seidel, A. Schulz, M.H.M. Sauer, J. Phys. Chem. 100 (1996) 5541.
[9] F.P. Schmidtchen, M. Berger, Chem. Rev. 97 (1997) 1609.

[10] C. Fu, L. Song, Y. Fang, Anal. Chim. Acta 399 (1999) 259.
[11] I. Capek, Adv. Colloid Interf. Sci. 97 (2002) 91.
[12] Y. Kubota, I. Motoda, Y. Shygemune, Y. Fujisaki, Photochem. Photobiol. 29 (1979) 1099.
[13] Y. Kubota, Y. Motoda, J. Phys. Chem. 84 (1980) 2855.
[14] G. Lober, L. Kittler, Stud. Biophys. 73 (1978) 25.
[15] L. Kittler, G. Lober, F.A. Gollmick, H. Berg, Bioelectrochem. Bioenerg. 7 (1980) 503.
[16] N.E. Geacintov, J.M. Prusikand, M.N. Khosrofian, J. Am. Chem. Soc. 98 (1976) 6444.
[17] N.E. Geacintov, R. Zhao, V.A. Kuzmin, S.K. Kim, L. Pecora, J. Photochem. Photobiol. 58 (1993) 185.
[18] M.V. Encinas, E.A. Lissi, Chem. Phys. Lett. 91 (1982) 55.
[19] M.V. Encinas, W.A. Rubio, E.A. Lissi, Photochem. Photobiol. 37 (1983) 125.
[20] M.H. Gehelen, F.C. de Schryver, Chem. Rev. 93 (1993) 199.
[21] R.S. Sarpal, S.K. Dogra, J. Photochem. Photobiol. A: Chem. 88 (1995) 147.
[22] S.K. Saha, G. Krishnamoorthy, S.K. Dogra, J. Photochem. Photobiol. A: Chem. 121 (1999) 191.
[23] T. Shanmugapriya, C. Selvaraju, P. Ramamurthy, Spectrochim. Acta A 66 (2007) 761.
[24] P. Lianos, R. Zana, J. Phys. Chem. 84 (1980) 3339.
[25] P. Lianos, R. Zana, J. Phys. Chem. 87 (1983) 1289.
[26] P. Lianos, M.L. Viriot, R. Zana, R. J. Phys. Chem. 88 (1984) 1098.
[27] I.R. Gould, P.L. Kuo, N.J. Turro, J. Phys. Chem. 89 (1985) 3030.
[28] C. Yihwa, M. Kellerman, M. Becherer, A. Hirsh, C. Bohne, Photochem. Photobiol. Sci. 6 (2007) 525.
[29] F. Lopez, F. Cuomo, A. Ceglie, L. Ambrosone, G. Palazzo, J. Phys. Chem. B 112 (2008) 7338.
[30] N. Yoshida, Y. Moroi, R. Humphrry-Baker, M. Grätzel, J. Phys. Chem. A 106 (2002) 3991.
[31] J.R. Hunter, Zeta Potential in Colloid Science, Accedemic Press, London, 1981 (Chapter 3).
[32] M. Ohtani, Y. Masuko, T. Wada, T. Kodama, Nucleic Acid Symp. 44 (2000) 51.
[33] P. Lianos, S. Georghiu, Photochem. Photobiol. 29 (1979) 13.
[34] V.Y. Shafirovich, S.H. Courtney, N. Ya, N.E. Geacintov, J. Am. Chem. Soc. 117 (1995) 4920.
[35] A. Okamoto, Y. Saito, I. Saito, J. Photochem. Photobiol. C 6 (2005) 108.
[36] M. Manoharan, K.L. Tivel, M. Zhao, K. Nafisi, T.M. Netzel, J. Phys. Chem. 99 (1995) 17461.
[37] R. Zana, Surfactant Solutions, vol. 22, in: R. Zana (Ed.), New York (Chapter 5), p. 241.
[38] C.A. Bunton, F. Nome, F.H. Quina, L.S. Romsted, Acc. Chem. Res. 24 (1991) 357 (and references therein).
[39] M.D. Reboiras, M. Kaszuba, M.T. Connah, M.N. Jones, Langmuir 17 (2001) 5314.